Distribution-based scaling to improve usability of regional climate model projections for hydrological climate change impacts studies

Wei Yang, Johan Andréasson, L. Phil Graham, Jonas Olsson, Jörgen Rosberg and Fredrik Wetterhall

ABSTRACT

As climate change could have considerable influence on hydrology and corresponding water management, appropriate climate change inputs should be used for assessing future impacts. Although the performance of regional climate models (RCMs) has improved over time, systematic model biases still constrain the direct use of RCM output for hydrological impact studies. To address this, a distribution-based scaling (DBS) approach was developed that adjusts precipitation and temperature from RCMs to better reflect observations. Statistical properties, such as daily mean, standard deviation, distribution and frequency of precipitation days, were much improved for control periods compared to direct RCM output. DBS-adjusted precipitation and temperature from two IPCC Special Report on Emissions Scenarios (SRESA1B) transient climate projections were used as inputs to the HBV hydrological model for several river basins in Sweden for the period 1961–2100. Hydrological results using DBS were compared to results with the widely-used delta change (DC) approach for impact studies. The general signal of a warmer and wetter climate was obtained using both approaches, but use of DBS identified differences between the two projections that were not seen with DC. The DBS approach is thought to better preserve the future variability produced by the RCM, improving usability for climate change impact studies.

Key words | climate change, downscaling, hydrological impacts

Wei Yang (corresponding author)
Johan Andréasson
L. Phil Graham
Jonas Olsson
Jörgen Rosberg
Swedish Meteorological and Hydrological Institute,
SE-60176, Norrköping,
Sweden
E-mail: *Wei.Yang@smhi.se*

Fredrik Wetterhall
Department of Geography,
King's College London,
Strand, London,
UK

NOMENCLATURE

DBS	Distribution-based scaling approach
DC	Delta change approach
ECHAM5	The EC Hamburg global climate model, version 5
GCM	Global climate model
HBV	Hydrological modelling developed at SMHI
IPCC	Intergovernmental Panel on Climate Change
MLE	Maximum likelihood estimator
MOS	Model output statistics
P	Precipitation
Q	River runoff (expressed here as $m^3 s^{-1}$)
RCA3	Rossby Centre Atmospheric model, version 3
$R3E5A1B_1$	Ensemble 1 of RCA3 projection with ECHAM5 global boundary conditions using SRES-A1B
$R3E5A1B_3$	Ensemble 3 of RCA3 projection with ECHAM5 global boundary conditions using SRES-A1B
RCM	Regional climate model
SRES-A1B	SRES future emissions scenario A1B
SRES	IPCC Special Report on Emissions Scenarios
T	Temperature

doi: 10.2166/nh.2010.004

INTRODUCTION

Global warming caused by an anthropogenic increase of greenhouse gases has already influenced present climate (IPCC 2007). This is likely to have even more impact if these gases continue to increase with future human activities. In the context of hydrology, the changing climate will likely accelerate the hydrological cycle on a global scale, and subsequently intensify the uneven distribution of hydrological resources (Trenberth 1999; Huntington 2006). This will in turn affect planning and management of water resources and associated infrastructure. Thus, assessment of climate change impacts on hydrological and meteorological variables on both regional and local scales is crucial.

The best tools to estimate future climate change at a global scale are global climate models (GCMs). They are developed to simulate the complex interactions between atmosphere, ocean and biosphere. Under assumptions of how the concentration of greenhouse gases change in the future, GCMs can be used to estimate the future evolution of climate. However, the coarse horizontal resolution of GCMs (~200–300 km) limits the direct use of their outputs in impact models such as catchment-based hydrological models, which are typically used at scales of 10–50 km. The large mismatch between the GCM scale and impacts scale must be addressed, and the most commonly used approach is downscaling.

Dynamical downscaling is one method to transfer information from GCMs to finer scales. It is usually carried out by applying a higher resolution regional climate model (RCM) over a limited area with boundary conditions from an overlying GCM. In comparison with GCMs, RCMs normally perform better at representing local climate, mainly due to (1) a better representation of geographical features such as orography due to the finer spatial resolution (~25–50 km) and (2) a better description of the physical processes by means of e.g. sub-grid scale parameterization and more detailed land surface schemes (Giorgi & Marinucci 1996; Hagemann *et al.* 2009). Furthermore, the most current use of RCMs with transient mode simulations makes it possible to investigate the evolution of climate change in a continuous manner, in contrast to the time-slice approach often used in earlier climate change impact studies (Kjellström *et al.* 2006).

In both GCM and RCM climate projections, a historical control period is defined (typically 1961–1990). This period represents only a possible realization of climate that should not be expected to match exactly with observations. What should match during this period, however, is the historical concentration of greenhouse gases in the atmosphere. Thus, the results do not represent the day-to-day evolution of observed weather but climate statistics such as seasonal, monthly and daily mean and standard deviations should be realistically reproduced for decadal scales (e.g. 30 year time periods). Even so, there is often a clear bias in the RCM statistics of key hydrometeorological variables such as precipitation and temperature (Kotlarski *et al.* 2005; Kay *et al.* 2006). Many of these biases originate from either the driving GCM or parameterizations in the RCM. Mismatch in scale between climate model and impact model can also produce model biases (Graham *et al.* 2007*a*). Direct use of RCM outputs in impact studies is therefore often not appropriate. Hydrologically important variables such as precipitation and temperature need to be adjusted to obtain realistic time series for use in local impact studies (Graham *et al.* 2007*b*).

One conventional way to construct precipitation and temperature time series for a future climate is to perturb an observed data series with a projected future climate change (e.g. Lettenmaier *et al.* 1999; Middelkoop *et al.* 2001). This is commonly known as the delta change (DC) approach (Hay *et al.* 2000). The long-term mean changes are calculated on a monthly or seasonal basis and added to the observation records. The same change is typically added to the entire frequency distribution, i.e. both for extreme and normal values, but the change can also be added as a function of the magnitude of the variable (e.g. Olsson *et al.* 2009). One disadvantage of this approach is the inability to deal with covariance and variability of the weather variables. The variance in future climate is kept the same as under present climate, which will likely not be true. The covariation between weather variables further disappears when the DC approach is implemented to each variable separately.

Another way to adjust future time series is referred to as bias correction (Lenderink *et al.* 2007). Correction factors are derived by comparing the RCM output with observed weather variables in the control period and then

applied to RCM output for future climate. In meteorology this is known as model output statistics (MOS) and has been used extensively to correct forecasts. Compared to the delta approach, the bias correction approach is also easy to implement but it further preserves the variability described by different climatic conditions generated by RCM projections. One disadvantage is the common assumption that the correction factors do not change with changing climate.

This paper presents an approach denoted *distribution-based scaling* (DBS) for adjusting RCM outputs for use in hydrological impacts models. The DBS approach aims to maximize utilization of RCM outputs to obtain more realistic input data for hydrological studies. It takes the covariance between precipitation and temperature into account. It reproduces the variations generated from the RCM-projected climate evolution and preserves them in adjustments to the key hydro-meteorological variables: precipitation and temperature. DBS was applied to hydrological modelling in river basins over Sweden. Two transient climate projections were used, which are ensemble members of the IPCC Special Report on Emissions Scenarios (SRES-A1B) performed with the EC Hamburg global climate model, version 5 (ECHAM5) GCM and downscaled with the Rossby Centre Atmospheric model, version 3 (RCA3) RCM. Three basins – Stenudden, Gimdalsby and Möckeln – were selected as examples to show how the DBS approach performs. For Stenudden, both the DBS and the DC approaches were applied and compared.

DATA AND METHODS

Study areas and observations

A gridded dataset of observed precipitation and temperature covering all of Sweden with a spatial resolution of 4 × 4 km was used as the baseline in the scaling procedure. It is calculated from the Swedish network of observation stations using optimal interpolation (Johansson 2000). Observations are adjusted according to effects from topography, wind direction and wind speed (Johansson & Chen 2003, 2005). The dataset starts in 1961 and is updated to the present day. For this study, the period 1961–1990 was used for baseline conditions.

Three river basins were used as case studies for validating the performance of the DBS approach: the Stenudden basin in the upper part of the Pite River; the Gimdalsby basin, a part of the Gimån River and the largest tributary to the Ljungan River; and the Möckeln basin, a part of the Helge River (Figure 1). The basins are situated in northern, central and southern Sweden respectively, representing different climatic and hydrological conditions (Table 1).

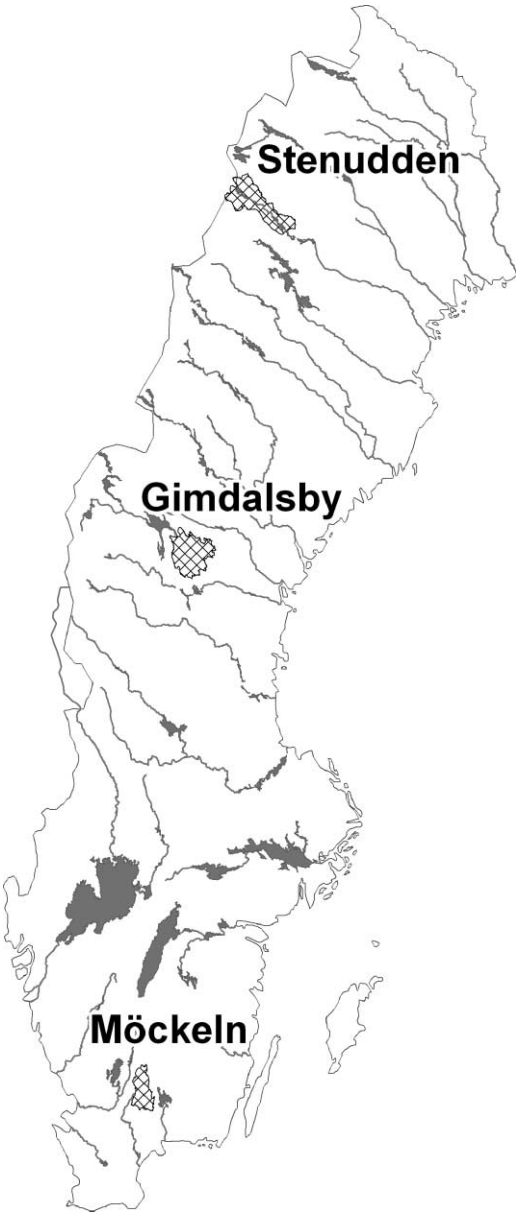

Figure 1 | The locations of Swedish river basins Stenudden, Gimdalsby and Möckeln used in this study.

Table 1 | Description of the study basins Stenudden, Gimdalsby and Möckeln

	Stenudden	Gimdalsby	Möckeln
Basin area (km^2)	2,400	2,200	1,000
Elevation range {mean} (m.a.s.l.)	450–700 {800}	260–520 {360}	140–210 {160}
Mean annual precipitation (mm)	852	610	752
Mean annual temperature (°C)	−3.0	1.9	6.2
Land cover (%)	Forest: 28.5; alpine: 58.4; glacier: 1.6; lake: 11.5	Forest: 80; open land: 10; lake: 10	Forest: 60; open land: 30; lake: 10

Many of the river basins in northern Sweden have their annual maximum peak flow during the spring flood. Biases in precipitation and temperature in winter and early spring can create large hydrological modelling errors in the accumulation of snow and subsequent snowmelt. Good model representation of the spring flood is important for these northern rivers to estimate flood risk and to efficiently plan production of electricity from the hydropower plants. Further south, a correct description of summer precipitation and temperature is also important to reproduce low flows causing droughts in southern river basins. For such reasons, adjustment for biases in the RCM outputs is necessary before they can be used in hydrological impact studies.

RCM projections

Regional climate projections for Europe were provided by the Rossby Centre Atmospheric Model, RCA3 (Kjellström *et al.* 2006). Two RCM projections, R3E5A1B$_1$ and R3E5A1B$_3$ based on the ECHAM5 GCM (Roeckner *et al.* 2006) were used in this study. They were created with the same RCM and based on the same emissions scenario, but the boundary GCM used two different initial conditions. This results in two separate outcomes, even although the assumed future anthropogenic conditions are the same. Assumptions for the future greenhouse gas concentrations follow the emissions scenario SRES-A1B, which is an intermediate scenario with respect to the magnitude of future global warming (Nakićenović *et al.* 2000). The RCA3 model domain used in this study covers all of Europe at a resolution of approximately 50 × 50 km.

Hydrological modelling

The HBV model was used for the hydrological modelling (Bergström 1995; Lindström *et al.* 1997). It is a conceptual semi-distributed rainfall-runoff model originally developed at the Swedish Meteorological and Hydrological Institute (SMHI) for operational runoff forecasting. It has also been used extensively to perform impact studies for climate change assessments (Vehviläinen & Huttunen 1997; Bergström *et al.* 2001; Andréasson *et al.* 2004; Graham 2004; Arheimer *et al.* 2005; Graham *et al.* 2007*a*, 2007*b*). The model is usually run on a daily time step and includes routines for snow accumulation and snowmelt, soil moisture, groundwater response and river routing. Input data include precipitation, temperature and potential evapotranspiration. A routing scheme connects runoff from different sub-basins. The model is calibrated against observed discharge, typically with the help of an automatic calibration routine to obtain optimal performance in terms of both short-term dynamics and long-term volumes. There are different options for estimating evapotranspiration in the HBV model; for this study, a temperature index method was used.

Experimental set-up

Total precipitation and air temperature at 2 m, hereafter often referred to as P and T, were extracted from the two RCA3 projections. To adjust the raw RCA3 output, the time series in the control periods (1961–1990) were scaled to match observed statistics using the DBS approach (discussed below). For simplicity, only the results from the R3E5A1B$_3$ projection are shown in this paper to illustrate the improvements in P and T after adjustment, compared to the raw RCA3 outputs. The DBS-adjusted control period results from R3E5A1B$_1$ are quite similar.

The DBS adjustment parameters obtained from the control periods were then applied to P and T for the future periods in the projections, to be used in the hydrological

modelling. DC factors were also estimated from the raw RCA3 output in future periods and applied to the baseline observations for 1961–1990 to create DC-perturbed datasets. The transient projections were divided into three time periods: 2011–2040, 2041–2070 and 2071–2100. This is a necessity for the DC approach and is also useful for analyzing the progression of climate change and its influence on P and T in near, intermediate and distant futures.

The adjusted P and T datasets were then used as inputs to the HBV model for numerous river basins in Sweden to create projected hydrological impacts from both the DBS and DC approaches. This paper focuses on results from the Stenudden basin as an example for how the two different approaches influence local hydrology. For comparison, resulting statistics of estimated P, T and Q (river runoff) were calculated both in the control period and in the future periods.

As there are many steps involved in the process of converting from climate modelling to assessment of hydrological impacts, Figure 2 shows a schematic with an overall summary of the main components. This general scheme provides a guideline whereby different emissions scenarios, GCMs, RCMs, ensemble projections, etc. can be used according to the availability of data or specific study needs.

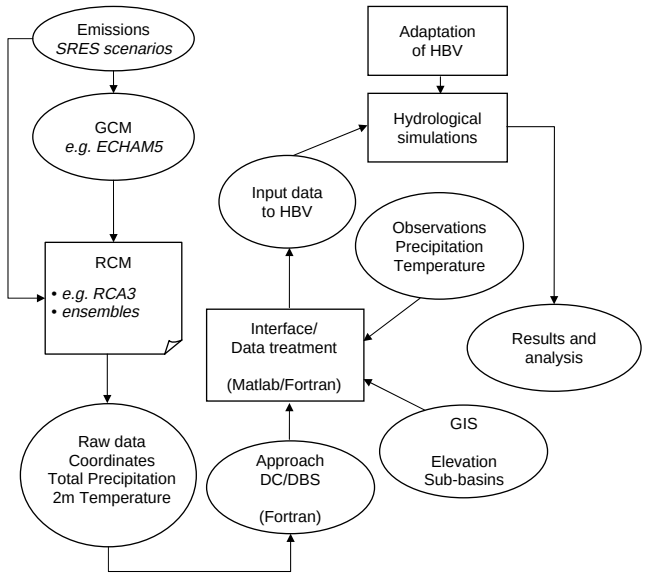

Figure 2 | Schematic plot of application procedure for using RCM projections in hydrological climate change impact studies.

METHODOLOGY DEVELOPMENT

Daily precipitation and temperature were the two variables to be adjusted in this study. It was assumed that simulations generated by RCA3 for the control period cover the full range of climate processes and events that occur in present climate, and is thus representative of present climate conditions. For the DBS approach, data in the control period are therefore assumed adequate for estimating scaling parameters against observations. For the future climate, precipitation and temperature were adjusted by the same DBS scaling factors derived in the control period for the respective climate projections.

DC approach

In the DC approach, only the climate change signal between the control period and a future time period was derived from the RCA3 time series of precipitation and temperature. This change was then applied to observations to create a perturbed time series representing the future time period. For precipitation, the percent change was derived as DC factors for the mean precipitation in each month. The daily precipitation in the observations was then multiplied by the respective monthly DC factors to produce the adjusted time series.

For temperature, a more detailed approach was used since the predicted changes can be considerably different at high and low temperature (Andréasson *et al.* 2004). The absolute change for each month was expressed by coefficients from a linear regression on the RCA3 control and future time series. The regression was made on the change between future and control periods against the control period temperature. The adjustment was conducted in two steps. First, the regression relationships were derived from daily control and future period temperatures from RCA3 as:

$$T_{\mathrm{fut}} = T_{\mathrm{ctl}} + a_{\mathrm{m}} + b_{\mathrm{m}}{}^{*}T_{\mathrm{ctl}} \quad (1)$$

where T_{fut} is the RCA3 future daily temperature, T_{ctl} is the RCA3 control daily temperature, m is the month and a and b are regression coefficients.

Secondly, the temperature for each day in the observations was adjusted according to the linear regression coefficients obtained from Equation (1) as:

$$T_{DC} = T_{obs} + a_m + b_m{}^{*} T_{obs} \quad (2)$$

where T_{DC} is the DC-adjusted daily temperature, T_{obs} is the observed daily temperature, m is the month and a and b are the regression coefficients derived in Equation (1).

Since changes were applied to daily values, a further adjustment was made to ensure that the resulting annual changes in both precipitation and temperature matched annual changes from the raw RCA3 outputs. Differences were typically small and adjustments were simply distributed evenly over the year so that the final annual change matched.

DBS approach for precipitation

In the case of precipitation, the DBS approach used two steps: (1) spurious drizzle generated by the RCA3 model was removed to obtain the correct percentage of wet days and (2) the remaining precipitation was transformed to match the observed frequency distribution. To obtain the percentage of wet days correctly, a cut-off value was identified for each sub-basin and season. Simulated and observed daily precipitation was sorted in descending order. The cut-off value was then defined as the threshold that reduced the percentage of wet days in the simulation to that of the observations. Days with precipitation amount larger than the threshold value were considered as wet days and all other days as dry days.

There are various theoretical distributions available to describe the probability distribution function (PDF) of precipitation intensities. A commonly used distribution is the gamma distribution, because of its ability to represent the typically asymmetrical and positively skewed distribution of daily precipitation intensities (Wilks 1995; Haylock *et al.* 2006; Yang *et al.* 2008). A single gamma distribution was therefore considered as the first choice in the DBS method, but then expanded as discussed below. The gamma distribution is a two-parameter distribution whose density distribution is expressed as:

$$f(x) = \frac{(x/\beta)^{\alpha-1} \exp(-x/\beta)}{\beta \Gamma(x)} \quad x, \alpha, \beta > 0 \quad (3)$$

where α is the shape parameter, β is the scale parameter and $\Gamma(x)$ is the inverse gamma function. The distribution parameters were estimated using maximum likelihood estimation (MLE).

Daily precipitation distributions are typically heavily skewed towards low-intensity values. As a result, the distribution parameters will be dominated by the most frequently occurring values, but may not be able to accurately describe the properties of extreme values. To capture the main properties of normal precipitation as well as extremes, the precipitation distribution was divided into two partitions separated by the 95th percentile. The resulting distribution is hereafter referred to as the double gamma distribution. Two sets of parameters – α, β and α_{95}, β_{95} – were estimated from observations and the RCA3 output in the control period (1961–1990). These parameter sets were in turn used to correct the RCA3 outputs for the entire projection period up to 2100 using the equation:

$$\begin{cases} P_{DBS} = F^{-1}(\alpha_{Obs}, \beta_{Obs}, F^{-1}(P, \alpha_{CTL}, \beta_{CTL})) & \text{if } P < 95^{th} \text{ percentile value} \\ P_{DBS} = F^{-1}(\alpha_{Obs,95}, \beta_{Obs,95}, F^{-1}(P, \alpha_{CTL,95}, \beta_{CTL,95})) & \text{if } P \geq 95^{th} \text{ percentile value} \end{cases} \quad (4)$$

where Obs denotes parameters estimated from observations and CTL denotes parameters estimated from the RCA3 output in the control period. F represents the gamma probability distribution.

The DBS parameters for daily precipitation were optimized separately for each sub-basin to preserve spatial variability of the RCA3 outputs. To take seasonal dependencies into account, they were also optimized for each season: DJF (Dec–Feb), MAM (Mar–May), JJA (Jun–Aug) and SON (Sep–Nov).

DBS approach for temperature

Compared to precipitation, temperature is more symmetrically distributed. It can be accurately described by a normal distribution with mean μ and standard deviation σ:

$$f(x) = \frac{1}{\sigma\sqrt{2\pi}} e^{-\left(\frac{x-\mu}{\sqrt{2}\sigma}\right)^2}. \quad (5)$$

The mean and standard deviation of daily temperature on a Julian day were smoothed over the control period using a 15-day moving window. Considering dependence between precipitation and temperature, temperature time series were described with distribution parameters conditioned by the wet or dry state of the day. Fourier series were used to smooth the seasonal mean and standard deviation of temperature for wet and dry days:

$$\mu\left(t^*_{\text{Dry/Wet}}\right) = \frac{a_{0,\text{Dry/Wet}}}{2} + \sum_{k=1}^{K}\left(a_{k,\text{Dry/Wet}} \cdot \cos\left(kwt^*\right) + b_{k,\text{Dry/Wet}} \cdot \sin\left(kwt^*\right)\right) \quad (6)$$

$$\sigma\left(t^*_{\text{Dry/Wet}}\right) = \frac{c_{0,\text{Dry/Wet}}}{2} + \sum_{k=1}^{K}\left(c_{k,\text{Dry/Wet}} \cdot \cos\left(kwt^*\right) + d_{k,\text{Dry/Wet}} \cdot \sin\left(kwt^*\right)\right). \quad (7)$$

where a_0, a_k, b_k, c_0, c_k and d_k are the Fourier coefficients, t^* is the day of the year; w equals $2\pi/n$, where n is the time units per cycle and k stands for the nth harmonic used for describing the annual cycle of adjusted daily temperature, T_{DBS}. Theoretically, $(t^*/2 + 1)$ harmonics are able to represent a complete cycle. Five harmonics were used and found to be sufficient.

The DBS parameters for temperature were calculated for both observations and RCM-simulated data series. They are denoted μ_{Obs}, σ_{Obs} and μ_{CTL}, σ_{CTL} and are used to scale the daily temperature:

$$T_{\text{DBS}} = F^{-1}(\sigma_{\text{Obs}}, \mu_{\text{Obs}}, F^{-1}(T_{\text{RCA}}, \sigma_{\text{CTL}}, \mu_{\text{CTL}})) \quad (8)$$

RESULTS AND DISCUSSION

Validation in the control period

In terms of mean basin precipitation, the control period outputs from the RCA3 model projections show a higher percentage of wet days and higher annual precipitation amounts in all three study basins (Table 2). The results are similar for both the R3E5A1B$_1$ and the R3E5A1B$_3$ projections. Annual overestimation for accumulated precipitation varies from 39% at Gimdalsby to 74% at Stenudden and for frequency of wet days varies from 14% at Stenudden to 33% at Gimdalsby. The biases in occurrence and volume differ from season to season, with the largest overestimation in spring and summer (Table 2). Observations show a higher number of dry days (i.e. days with no precipitation) and generally less precipitation in most intensity intervals, as shown in Figure 3. This is also apparent in the frequency distribution curves shown in Figure 4.

Table 2 | Precipitation characteristics of the raw outputs from the control period of the two RCA3 projections. The total accumulated precipitation (P_{acc}) is in mm; the frequency of occurrence (freq) is in %. Differences between observation and raw RCA3 outputs are expressed in % (ΔP_{acc}, Δfreq, in brackets)

		Stenudden		Gimdalsby		Möckeln	
		R3E5A1B$_1$	R3E5A1B$_3$	R3E5A1B$_1$	R3E5A1B$_3$	R3E5A1B$_1$	R3E5A1B$_3$
DJF	P_{acc} (ΔP_{acc})	258.4 (19.6)	264.0 (22.0)	145.6 (30.0)	155.0 (38.4)	221.5 (32.6)	225.0 (34.7)
	freq (Δfreq)	97.1 (8.7)	97.8 (9.5)	93.7 (26.8)	94.1 (27.3)	91.9 (17.8)	92.4 (18.5)
MAM	P_{acc} (ΔP_{acc})	307.1 (120.0)	280.0 (100.0)	177.2 (59.6)	175.0 (57.7)	227.4 (56.8)	212.0 (46.2)
	freq (Δfreq)	92.9 (21.9)	92.5 (21.4)	85.1 (43.1)	83.7 (40.9)	83.3 (29.8)	84.6 (31.8)
JJA	P_{acc} (ΔP_{acc})	476.2 (100.0)	475.0 (99.6)	299.1 (34.1)	278.0 (24.7)	385.2 (75.9)	370.0 (68.9)
	freq. (Δfreq)	96.7 (17.5)	96.9 (17.7)	95.3 (36.1)	94.5 (35.0)	95.7 (32.2)	95.7 (32.2)
SON	P_{acc} (ΔP_{acc})	441.4 (70.9)	411.0 (59.3)	239.5 (46.0)	237.0 (44.5)	310.4 (40.5)	296.0 (33.9)
	freq (Δfreq)	97.9 (9.8)	97.7 (9.7)	94.7 (27.1)	95.2 (27.8)	93.2 (19.2)	94.5 (20.8)
ANN	P_{acc} (ΔP_{acc})	1483.0 (74.0)	1430.0 (67.8)	861.4 (41.2)	845.0 (38.5)	1144.5 (52.2)	1103.0 (46.7)
	freq (Δfreq)	96.2 (14.3)	96.2 (14.3)	92.2 (32.9)	92.0 (32.6)	91.0 (24.5)	91.8 (25.6)

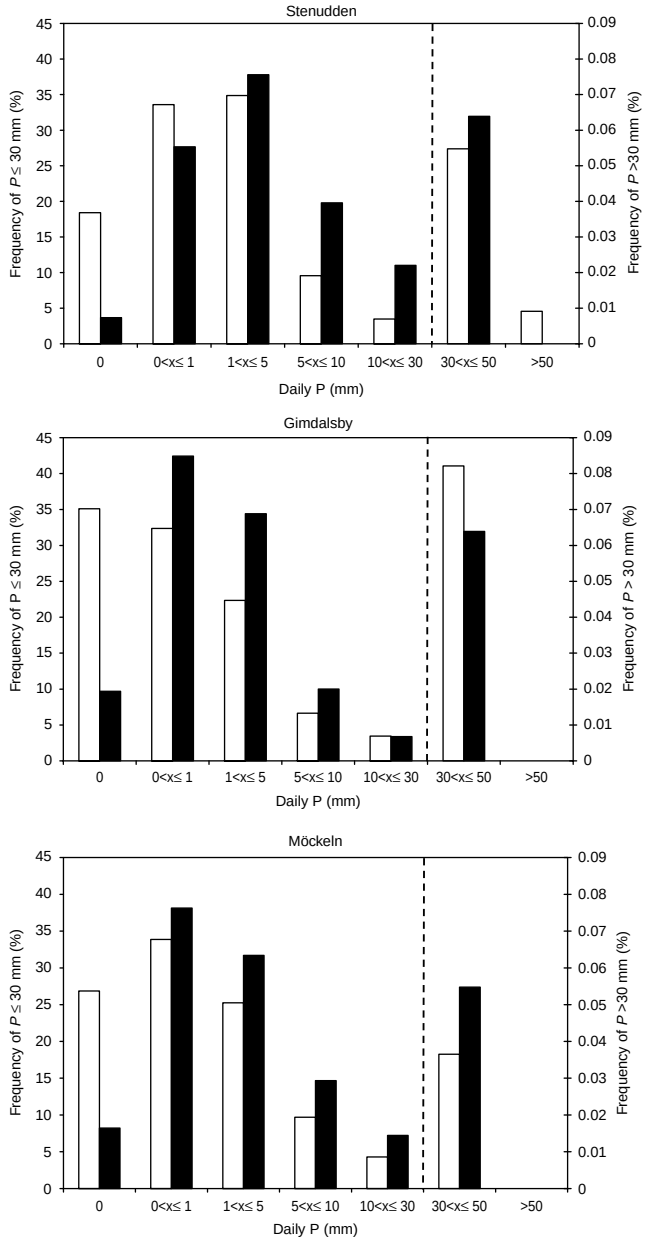

Figure 3 | Distribution of precipitation amounts from observations for 1961–1990 (white) and from the R3E5A1B$_3$ projection control period (black). Note that a different scale (right side, *y* axis) is used for the highest precipitation amounts (i.e. greater than 30 mm per day).

In terms of mean daily temperature, projection outputs from the RCA3 model show relatively good performance in reproducing the annual cycle, but the model generally underestimates temperature in summer and overestimates it in winter (Figure 5). This statement takes into account that wet days are more frequent for all of these basins and thus more representative of the overall mean. Seasonal biases are more pronounced for days without precipitation during the winter season, but for these days the model underestimated the temperature.

After applying the DBS approach, the large differences in rainfall frequency between the observation and simulation were reduced considerably (Figure 4). Use of the double gamma distribution reproduced rainfall of all magnitudes better than the single gamma distribution. In particular, the more extreme high precipitation intensities are better described, as seen in Figure 6. All results in the remaining figures are based on the double gamma distribution for precipitation scaling. As with daily precipitation, the DBS approach also considerably improved the modelled daily temperature in both mean and variability (Figure 7). The largest improvements are seen in the correction of the warm bias in winter, spring and autumn. The cold bias for high temperatures and warm bias for low temperatures in summer was also reduced.

Runoff and snow depth were simulated by the HBV model using observations, raw RCA3 outputs and DBS-adjusted RCA3 outputs for the control period (Figure 8). The geographical characteristics of pronounced spring peak flows in the northern part of Sweden to high winter flows and only a weak spring peak in the south are clearly exhibited by the runoff produced by observations. Although not shown here, runoff simulated with observed precipitation and temperature closely follows observed runoff in all catchments and can be used as a baseline for comparison. The runoff simulated from raw RCA3 precipitation and temperature deviates considerably from this baseline, showing large overestimation over the entire year. This was especially evident during the spring flood for the two northern catchments. The large runoff bias was almost entirely eliminated in the HBV model simulation using DBS-adjusted precipitation and temperature. Similarly, results for snow depth lie much closer to the baseline after DBS adjustment. Bias reduction is, on average, 90% for runoff and 87% for snow depth (Table 3).

Evaluation for future climate

Assessment for future hydrological impacts focused on the Stenudden basin. A warmer and wetter climate in the

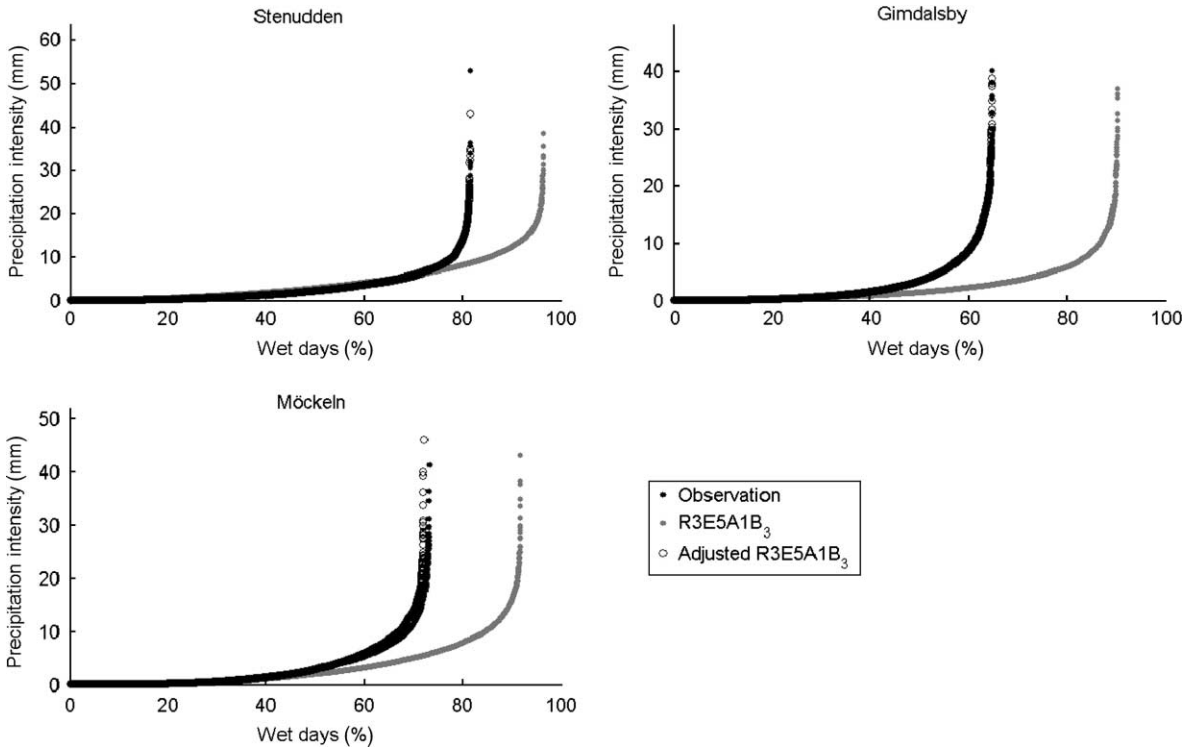

Figure 4 | Distribution of precipitation intensities for all three study basins calculated from observations (1961–1990) and raw R3E5A1B$_3$ output and DBS-adjusted R3E5A1B$_3$ output for the control period. Note that the observations are difficult to see as the DBS-adjusted values closely overlie them.

Stenudden basin can be expected for the future according to the two climate projections used (Table 4, Figure 9). Furthermore, use of the DBS approach shows more pronounced climate change signals in precipitation and temperature than for the DC approach.

One should bear in mind that the tendencies shown in Figure 9 tend to highlight results that occur for extreme values over the 95th percentile. This is caused by the scale of the plot in relation to the number of data points. Plots at different scales (not shown here) would allow more detailed analysis of the different populations of the results with regard to the two different gamma distributions used. The volume change with time shown in Table 4 is, however, more representative of the more frequent, lower magnitude events.

Due to the inherent differences in the two approaches, different datasets are shown in Figure 9 as the reference (i.e. x axis) for the DC and DBS approaches. In the DC approach, the future adjusted precipitation is compared with the observed precipitation from where it was derived. In the DBS approach, future adjusted precipitation is compared with adjusted precipitation for the control period, from where the scaling factors were derived. For comparison, future precipitation against control precipitation for raw outputs from the RCA3 projections is also shown.

The HBV-simulated runoff from Stenudden for the period 2011–2040 is quite similar to the control period, which indicates that nothing would change dramatically in the coming 30 years according to these projections (Figure 10). When moving towards the year 2100, the tendency is towards a warmer and wetter climate (Figures 11 and 12). Consequently, the results show increased runoff in HBV simulations using precipitation and temperature from both the DC and DBS approaches later in the century (Table 4). The increase in temperature causes an earlier start of the spring snowmelt flood. The annual peak flow tends to arrive earlier in spring, summer flows tend to decrease and autumn flows tend to increase (Figures 11 and 12).

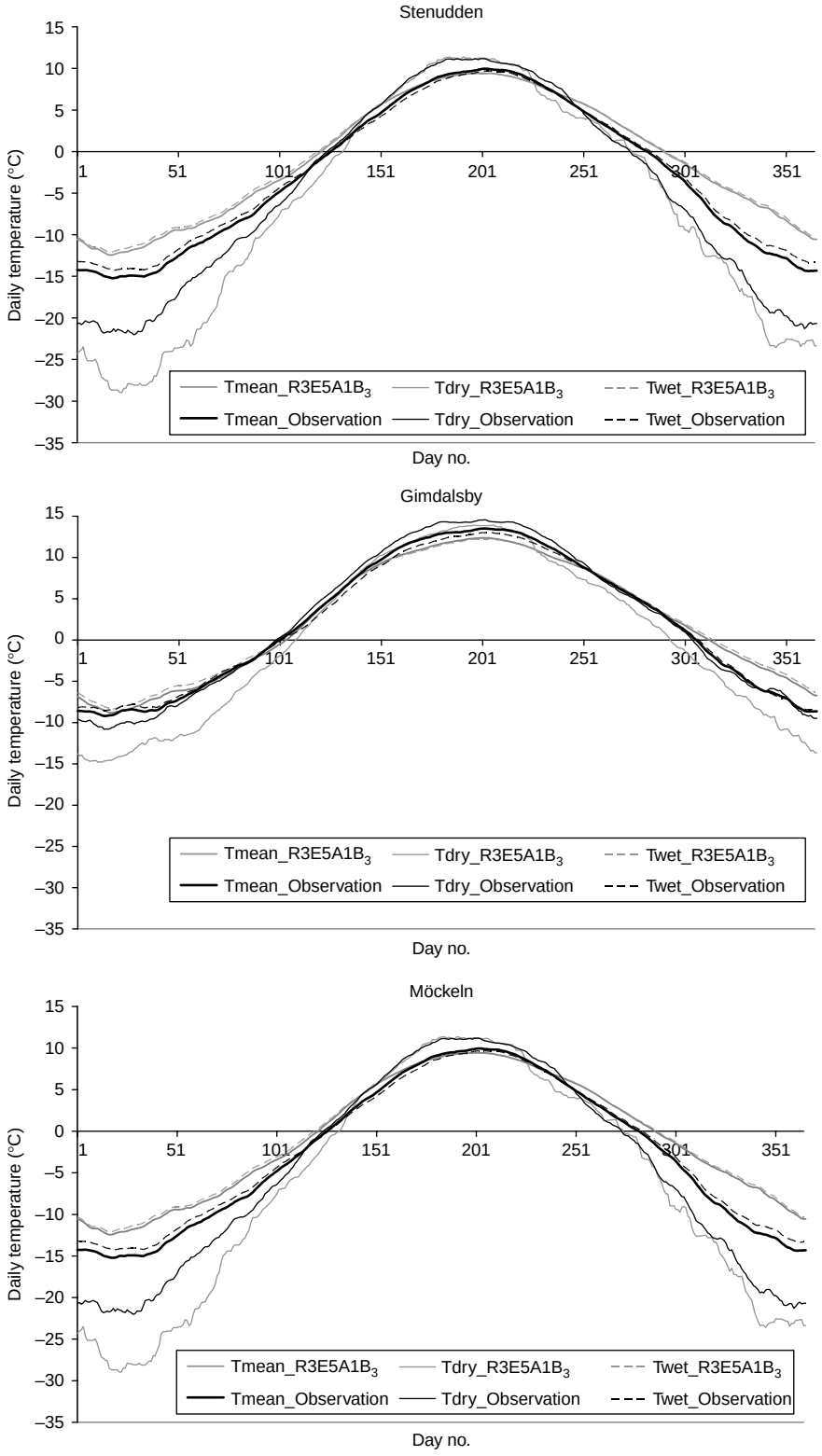

Figure 5 | Annual cycle of daily temperature from observations (1961–1990) and the R3E5A1B$_3$ projection for the control period (Tmean: mean daily temperature; Twet: mean daily temperature for days with precipitation; Tdry: mean daily temperature for dry days).

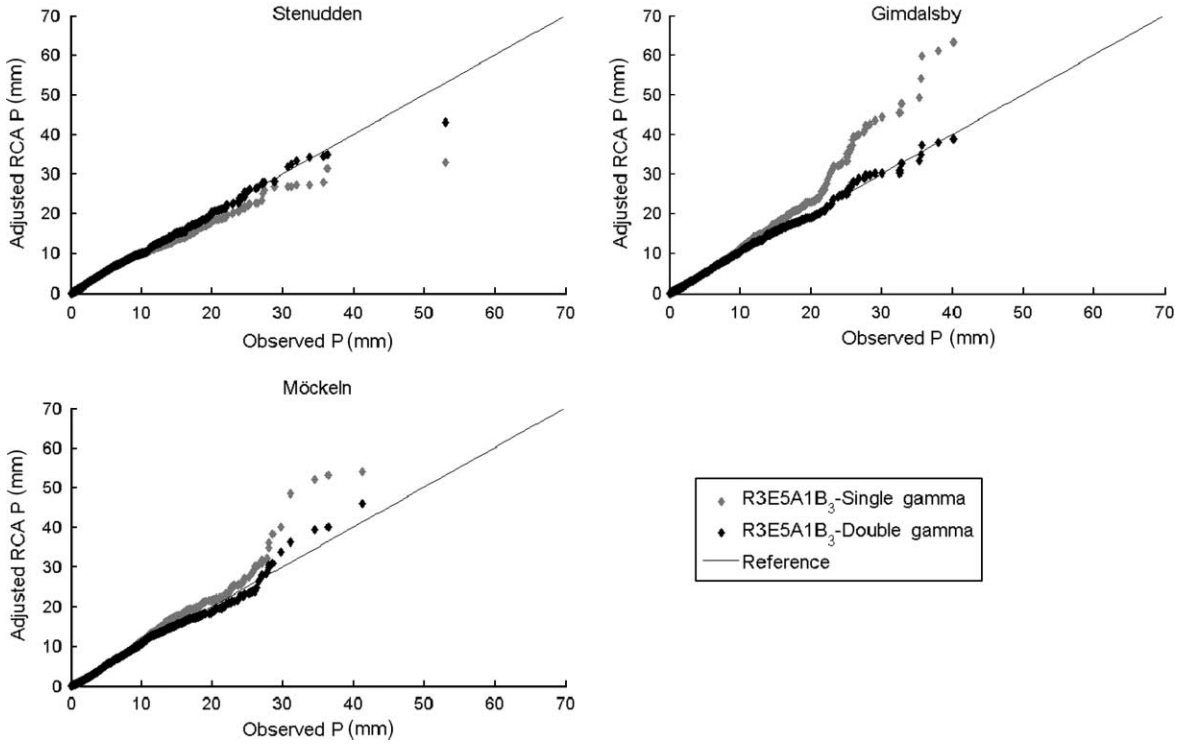

Figure 6 | Comparison of precipitation from observations (1961–1990) and from the DBS-adjusted R3E5A1B$_3$ projection using a single gamma distribution and a double gamma distribution for the control period in all three study basins.

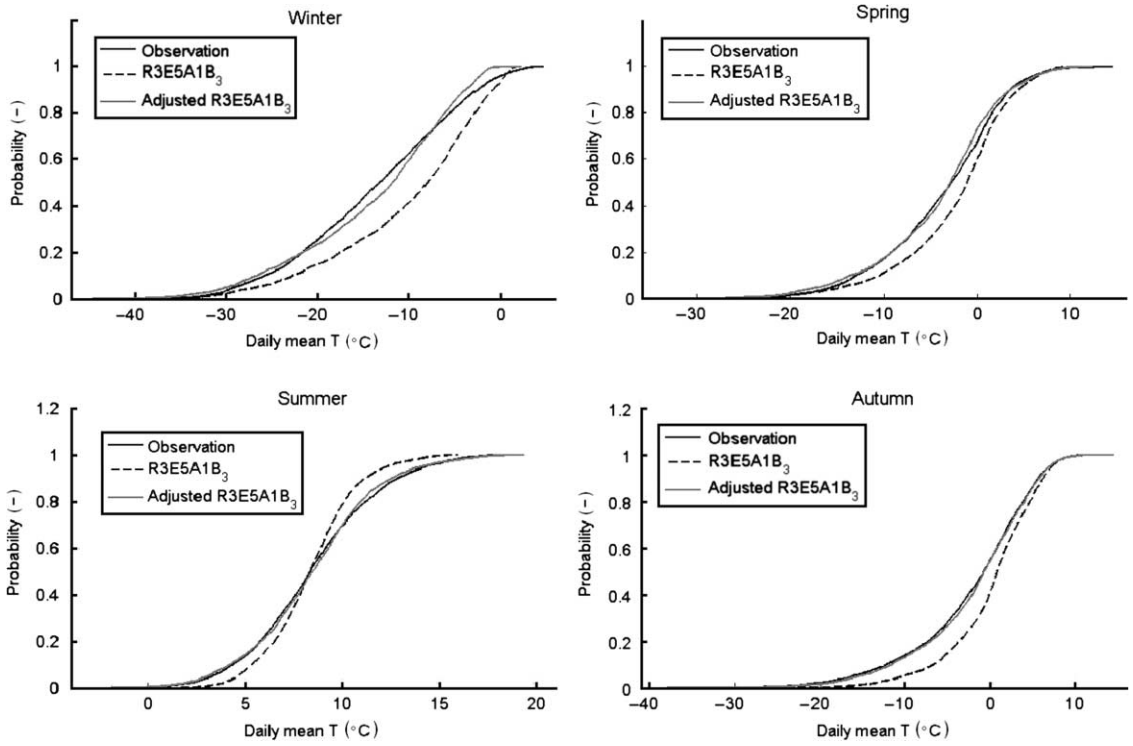

Figure 7 | Distribution of daily temperature from observations (1961–1990) and raw R3E5A1B$_3$ and DBS-adjusted R3E5A1B$_3$ projection outputs for the control period for each season in the Stenudden basin.

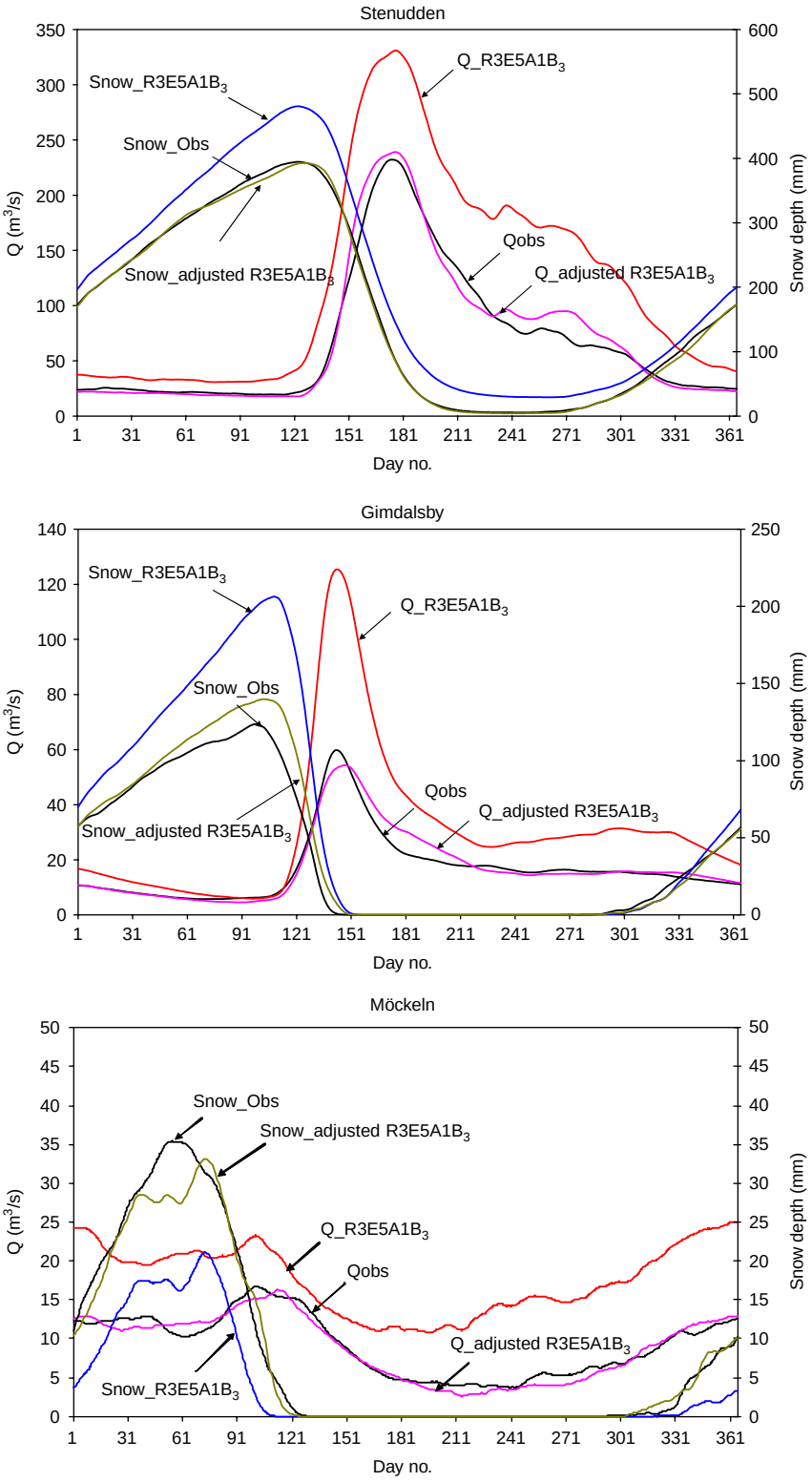

Figure 8 | Mean daily runoff *Q* and snow depth in all three study basins simulated with the HBV model using precipitation and temperature from observations (1961–1990) and raw R3E5A1B$_3$ and DBS-adjusted R3E5A1B$_3$ projection outputs for the control period.

Table 3 | Bias in HBV-simulated runoff and snow depth using raw and DBS-adjusted R3E5A1B$_3$ projection outputs

		Stenudden		Gimdalsby		Möckeln	
		Raw	DBS	Raw	DBS	Raw	DBS
R3E5A1B$_1$	Bias in runoff (%)	55.4	17.9	128.8	−0.2	37.7	−2.8
	Bias in snow depth (%)	18.6	0.9	57.7	5.1	−28.1	−7.6
R3E5A1B$_3$	Bias in runoff (%)	42.7	3.0	109.6	−9.2	49.5	−2.6
	Bias in snow depth (%)	21.8	−0.5	66.7	13.1	−40.5	−6.5

Response to climate model projection

The two climate projections result in somewhat different future climates, although the projections only differ in their initial conditions. Differences in trends between the two variables precipitation and temperature are apparent, as are differences in how these two variables respond over different time periods (Table 4).

For future temperature, equally warm tendencies are seen in both projections with a slight difference of 0.1–0.2°C between the projections for a given time period and adjustment approach. The major differences between the two projections are mainly reflected in the trend of future precipitation, particularly for the period 2011–2040. In R3E5A1B$_1$, the precipitation does not vary much over the projection period 2011–2040 and then shows an increasing trend for 2041–2100. In R3E5A1B$_3$ there is a clearer wet tendency starting in 2011. This difference between the two projections seen in the near future becomes smaller as the climate change signal becomes stronger towards the end of the century.

Runoff reacts consequently to the trends identified for precipitation and temperature. Different trends and magnitudes for relative changes of precipitation and temperature subsequently lead to contrasting estimates of runoff generated from the two projections. For the coming 30 years, average runoff shows a decrease in R3E5A1B$_1$ and an increase in R3E5A1B$_3$. For the intermediate to distant future, runoff increases in both projections. For the near future, the natural variability represented in the climate models appears to have a stronger signal than the climate change signal, at least for precipitation. As the climate evolves and responds to the effects of the emissions scenario, the climate change signal becomes stronger (Figures 10–12).

Response to adjustment approach

Given the same RCA3 projection, the DC and the DBS approaches produce different results for the future climate, in particular for precipitation (Table 4 and Figure 9). With the DC approach applied to precipitation, no clear difference is found between the projections for the same time period, although different climate change signals are apparent between different time periods. Except for the time period 2011–2040, the adjusted precipitation from both projections shows a similar linear response of precipitation with time towards 2100. As the same level of correction was applied to both the normal and extreme precipitation values, this may minimize the differences between different projections (Figures 9(e) and 9(f)). These results also indicate that the DC approach is more apt to address relative changes in mean rather than extreme events.

In contrast to the DC approach, a larger deviation from the control precipitation for the two projections can

Table 4 | Relative future changes in Stenudden basin for mean precipitation (ΔP), temperature (ΔT) and runoff (ΔQ), as compared with the control period for the two RCA3 projections and both adjustment approaches (DC and DBS)

		R3E5A1B$_1$		R3E5A1B$_3$	
Time period	Variable	DC	DBS	DC	DBS
2011–2040	ΔT (°C)	0.9	1.0	1.0	1.2
	ΔP (%)	0.3	−0.5	6.5	8.0
	ΔQ (%)	−0.9	−1.6	5.5	7.3
2041–2070	ΔT (°C)	2.4	2.8	2.5	3.0
	ΔP (%)	9.3	9.0	12.3	16.5
	ΔQ (%)	7.9	6.8	10.9	15.0
2071–2100	ΔT (°C)	3.9	4.6	3.9	4.6
	ΔP (%)	18.9	20.9	18.1	23.6
	ΔQ (%)	16.7	17.4	16.1	21.2

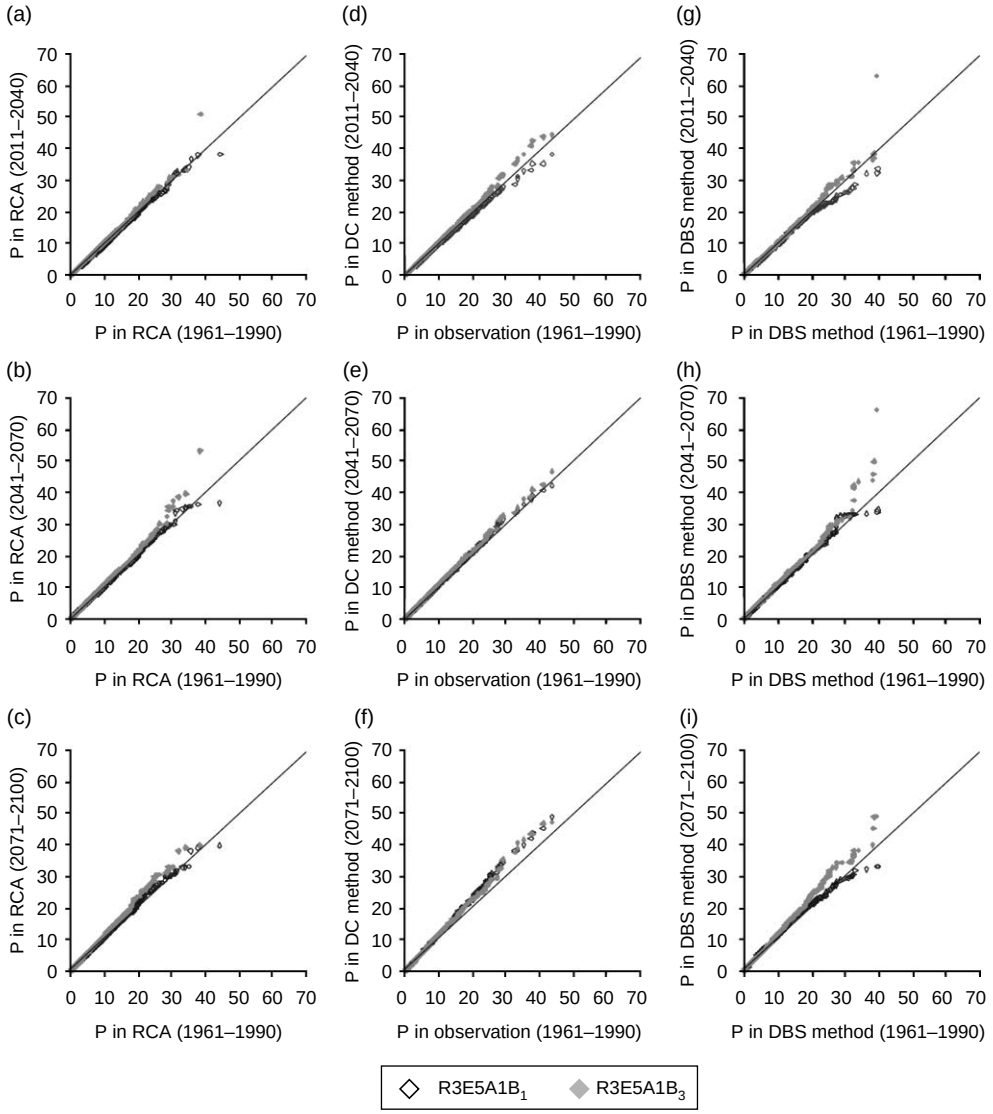

Figure 9 | Comparison between precipitation in the control or baseline period (*x* axis) and in future periods (*y* axis; 2011–2040 in the upper row, 2041–2070 in the middle row, 2071–2100 in the bottom row) for both the R3E5A1B$_1$ and R3E5A1B$_3$ projections in the Stenudden basin. The left column shows raw RCA3 outputs, the middle column shows DC-adjusted RCA3 outputs and the right column shows DBS-adjusted RCA3 outputs. The complete time series for each period are shown, sorted by magnitude.

be seen for the DBS approach. The adjusted DBS precipitation appears to preserve trends identified in the raw RCM outputs. It also captures variations in the extreme events in addition to the trend for the mean (Figures 9(h) and 9(i)).

The runoff generated for future time periods using adjusted precipitation and temperature also shows different patterns depending on the adjustment approach used (Figures 10–12), as expected from the precipitation results. Runoff obtained using the DC approach for the years up to 2070 is similar to the baseline. Although the annual peak flow occurs earlier, its magnitude does not exceed baseline conditions. A larger variation in flow for the winter and spring season occurs for the period 2071–2100 (Figure 12). Influence from the future climate onto hydrological conditions is more noticeable, even in earlier periods, using the DBS approach. In contrast to the DC approach, the peak flow decreased in the R3E5A1B$_1$ projection for 2011–2040, but increased in R3E5A1B$_3$. In both projections, the annual peak runoff tends to occur earlier, as with

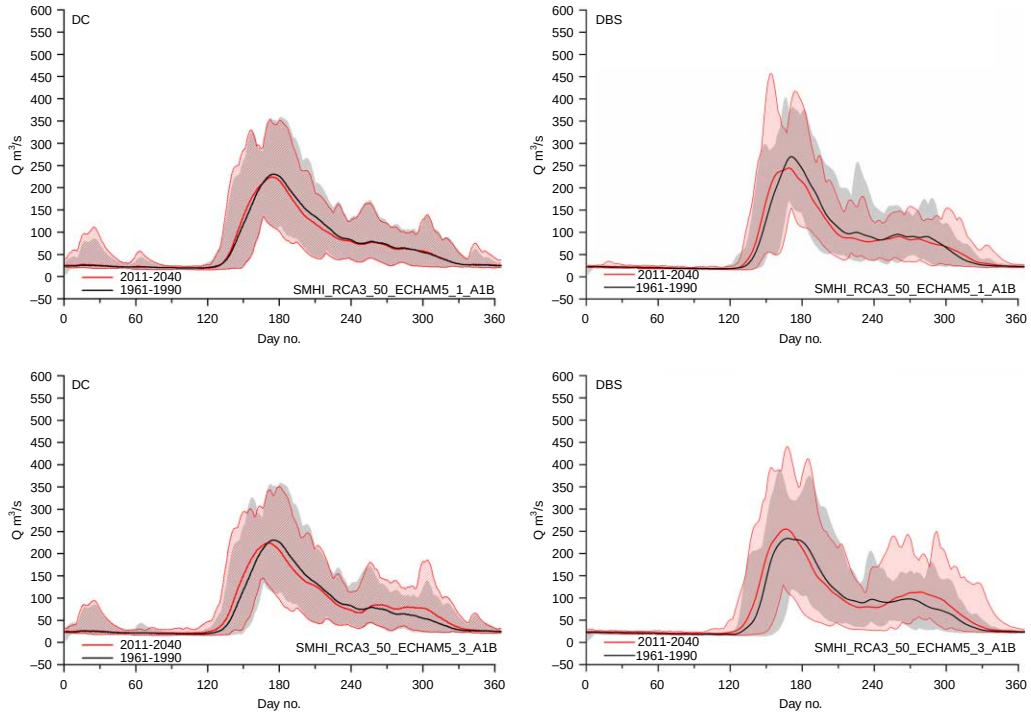

Figure 10 | Intra-annual runoff Q in the Stenudden basin simulated with the HBV model for 2011–2040 from the projections R3E5A1B$_1$ (upper) and R3E5A1B$_3$ (lower). Red shows the mean and range for the future period; black and grey show the mean and range for the control period. The left and right plots show results from the DC and DBS approaches, respectively. For the full colour version of this figure, subscribers should access the online version of the journal at http://www.iwaponline.com/nh/toc.htm

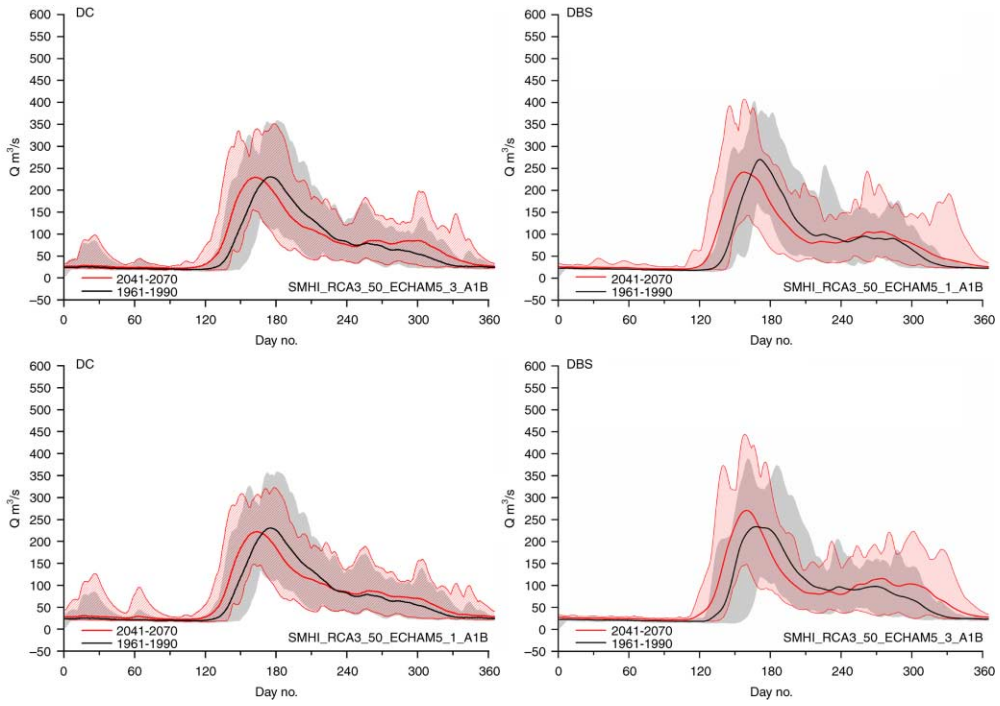

Figure 11 | Intra-annual runoff Q in the Stenudden basin simulated with the HBV model for 2041–2070 from the projections R3E5A1B$_1$ (upper) and R3E5A1B$_3$ (lower). Red shows the mean and range for the future period; black and grey show the mean and range for the control period. The left and right plots show results from the DC and DBS approaches, respectively. For the full colour version of this figure, subscribers should access the online version of the journal at http://www.iwaponline.com/nh/toc.htm

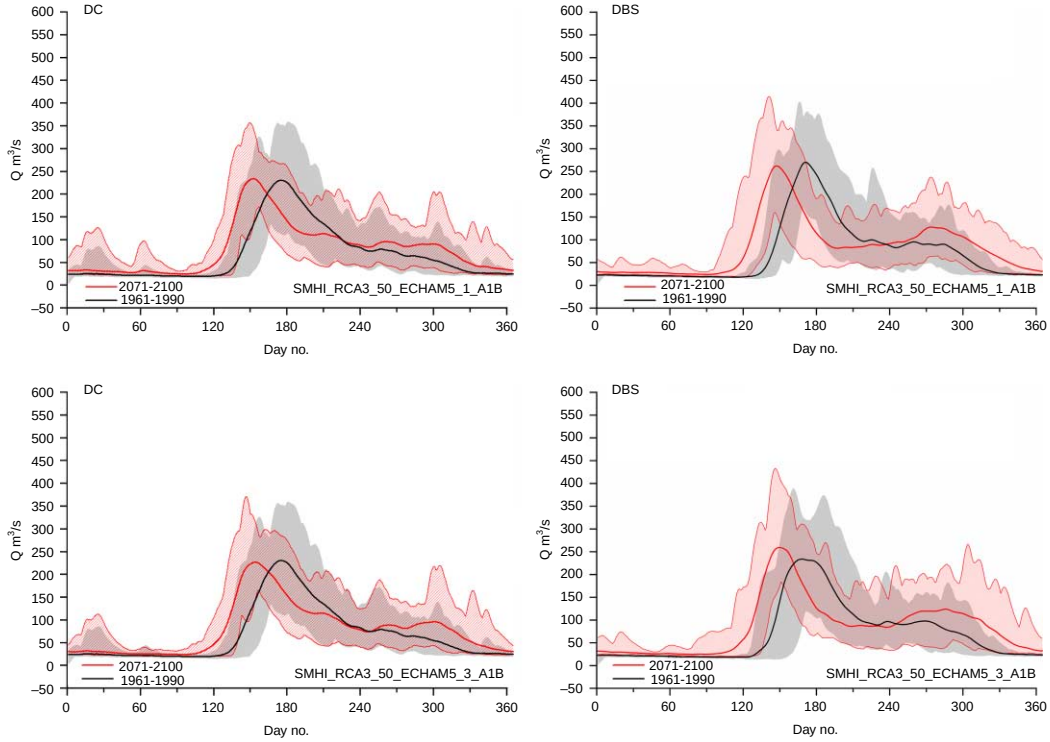

Figure 12 | Intra-annual runoff Q in the Stenudden basin simulated with the HBV model for 2071–2100 from the projections R3E5A1B$_1$ (upper) and R3E5A1B$_3$ (lower). Red shows the mean and range for the future period; black and grey show the mean and range for the control period. The left and right plots show results from the DC and DBS approaches, respectively. For the full colour version of this figure, subscribers should access the online version of the journal at http://www.iwaponline.com/nh/toc.htm

the DC approach. Differences in the response of peak flows are seen throughout the projected future period for the DBS approach, with R3E5A1B$_3$ generating increased peak flow and R3E5A1B$_1$ showing a decreased peak or little change.

Differences in the results between the two approaches can be explained in part by their underlying concepts. The DC approach transfers the average climate change signals onto observed variability, whereas the DBS approach is more influenced by the variability produced by individual RCM projections. The DC approach treats the relative changes for extreme events in the same way as for normal events, but the DBS approach treats them separately by associating them with different distributions. In terms of temperature, the DBS approach adjusts temperature time series differently conditioned on the wet or dry state of the day, which is determined by the adjustment of daily precipitation. This may explain why more pronounced climate change signals are seen with the DBS approach. In contrast, the DC approach makes no attempt to adjust the RCM outputs, but merely uses them to obtain the climate change signal.

Uncertainty in scaling approaches

One concern with scaling approaches is their strong dependence on the combined performance of the GCM and the downscaling RCM. The capability of the GCM/RCM combination to capture the major natural variability of the present climate will influence outputs. This is in contrast to the DC approach that offers a rather fixed representation of variability, but a robust representation of mean climate change. The scaling factors affect adjustment of climate variables for the future climate. The worse the performance of the climate models, the more effect the scaling procedure will have on the outcome. From this point of view, a large ensemble of RCM outputs driven by a GCM with different initial conditions and a selection of different emissions scenarios could help to further identify uncertainties from the paired GCM/RCM projections.

This would also provide a more complete analysis of climate change effects on local study areas along with greater insight on the range of model uncertainties.

A clear advantage of the DBS approach is removal of much of the systematic bias from the RCM and its paired GCM. This provides a climate change signal that is more related to the actual climate change rather than model artefacts. A large range in an ensemble of GCM/RCM projections is useful for estimating the uncertainty associated with climate change studies, but it is more beneficial if this reflects uncertainties regarding the climate processes rather than model biases.

CONCLUSIONS

This paper presents a general approach for adjusting RCM output for use in hydrological impact studies termed *distribution-based scaling* (DBS). The approach was applied to two hydro-meteorological variables, precipitation and temperature, and the performance was verified by hydrological modelling. The scaling uses a double gamma distribution for daily precipitation, partitioned into normal and extreme, and a normal distribution for daily temperature. Results using the DBS approach were compared to results using the delta change (DC) approach. The main conclusions from this work include the following.

- The inclusion of a second gamma distribution for rainfall events above the 95th percentile considerably improved reproduction of the full range of the precipitation distribution.
- The DBS approach produced a more realistic representation of local hydrology than by using raw RCM output, which consequently improved the modelled snow depth and timing of peak flow in spring in Sweden.
- The DC approach resulted in essentially identical signals for the two climate model ensemble projections. This shows that DC primarily transfers the main trends of the GCM/RCM combination and not the annual variability.
- The DBS approach reproduced different signals from the two climate model ensemble projections. This shows that DBS is more sensitive to the projections in use and preserved the annual variability from the corresponding GCM/RCM projection.
- The DBS approach uses projected climate variables in a transient (continuous) mode, a feature that is not possible with the DC approach.

Future outlook

Reliance on a single combination of GCM and RCM to represent the current climate and make future projections is not sufficient given the amount of uncertainty involved in the climate models themselves. The scaling approach and consequent hydrological modelling should be tested on an ensemble of different GCM/RCM projections to better assess uncertainty in the techniques. The resulting simulations of runoff would provide a more complete overview of the climate change effects on local study areas.

The DBS method will benefit from further development. As presented here, the 95th percentile was used to distinguish normal and extreme precipitation events. This was a fixed threshold for all projections and all study areas. Although this works well for most of the basins studied so far, a more flexible threshold may allow a better fit of the double gamma distribution to precipitation under varying circumstances, as proposed by Vrac *et al.* (2007). Another potential improvement for the DBS approach would be to use some type of classification system for identifying large-scale circulation patterns. This would enable the possibility to identify scaling factors for different types of precipitation events rather than treating them all equally.

Future applications will see finer resolutions used in climate models, both at global and regional scales. It remains to be seen how this will affect the magnitude of adjustments needed for hydrological applications. However, climate models will still be subject to systematic biases and the need to make corrections will likely continue into the foreseeable future.

ACKNOWLEDGEMENTS

This work was carried out under joint funding from the European ENSEMBLES Project (EU GOCE-CT-2003-505539), ELFORSK, Svenska Kraftnät, the Nordic Project on Climate and Energy Systems (Nordic Energy Research).

The RCA3 projections were performed by the Rossby Centre at SMHI with boundary conditions from ECHAM5 provided by the Max Planck Institute for Meteorology in Hamburg and the Danish Meteorological Institute in Copenhagen.

REFERENCES

Andréasson, J., Bergström, S., Carlsson, B., Graham, L. P. & Lindström, G. 2004 Hydrological change–climate change impact simulations for Sweden. *Ambio* **33**, 4–5.

Arheimer, B., Andréasson, J., Fogelberg, S., Johnsson, H., Pers, C. B. & Persson, K. 2005 Climate change impact on water quality: model results from southern Sweden. *Ambio* **34**, 559–566.

Bergström, S. 1995 The HBV model. In: Singh, V. P. (ed.) *Computer Models of Watershed Hydrology*. Water Resources Publications, Highlands Ranch, Colorado, pp. 443–476.

Bergström, S., Carlsson, B., Gardelin, M., Lindström, G., Pettersson, A. & Rummukainen, M. 2001 Climate change impacts on runoff in Sweden–assessments by global climate models, dynamical downscaling and hydrological modelling. *Clim. Res.* **16**, 101–112.

Giorgi, F. & Marinucci, M. R. 1996 Improvements in the simulation of surface climatology over the European region with a nested modelling system. *Geophys. Res. Lett.* **23**, 273–276.

Graham, L. P. 2004 Climate change effects on river flow to the Baltic Sea. *Ambio* **33**, 235–241.

Graham, L. P., Andréasson, J. & Carlsson, B. 2007*a* Assessing climate change impacts on hydrology from an ensemble of regional climate models, model scales and linking methods–a case study on the Lule River Basin. *Clim. Change* **81**, 293–307.

Graham, L. P., Hagemann, S., Jaun, S. & Beniston, M. 2007*b* On interpreting hydrological change from regional climate models. *Clim. Change* **81**, 97–122.

Hagemann, S., Göttel, H., Jacob, D., Lorenz, P. & Roeckner, E. 2009 Improved regional scale processes reflected in projected hydrological changes over large European catchments. *Clim. Dyn.* **32**, 767–781.

Hay, L. E., Wilby, R. L. & Leavesley, G. H. 2000 A comparison of delta change and downscaled GCM scenarios for three mountainous basins in the United States. *J. Am. Water Resour. Assoc.* **36**, 387–398.

Haylock, M. R., Cawley, G. C., Harpham, C., Wilby, R. L. & Goodess, C. M. 2006 Downscaling heavy precipitation over the United Kingdom: a comparison of dynamical and statistical methods and their future scenarios. *Int. J. Climatol.* **26**, 1397–1415.

Huntington, T. 2006 Evidence for intensification of the global water cycle: review and synthesis. *J. Hydrol.* **319**, 83–95.

IPCC 2007 In: Pachauri, R. K. & Reisinger, A. (eds) *Climate Change 2007: Synthesis Report. Contribution of Working Groups I, II and III to the Fourth Assessment Report of the Intergovernmental Panel on Climate Change*. IPCC, Geneva, Switzerland, p. 104.

Johansson, B. 2000 Areal precipitation and temperature in the Swedish mountains, an evaluation from a hydrological perspective. *Nordic Hydrol.* **31**, 207–228.

Johansson, B. & Chen, D. 2003 The influence of wind and topography on precipitation distribution in Sweden: statistical analysis and modelling. *Int. J. Climatol.* **23**, 1523–1535.

Johansson, B. & Chen, D. 2005 Estimation of areal precipitation for runoff modelling using wind data: a case study in Sweden. *Clim. Res.* **29**, 53–61.

Kay, A. L., Jones, R. G. & Reynard, N. S. 2006 RCM rainfall for UK flood frequency estimation. I. Method and validation. *J. Hydrol.* **318**, 151–162.

Kjellström, E., Bärring, L., Gollvik, S., Hansson, U., Jones, C., Samuelsson, P., Rummukainen, M., Ullerstig, A., Willén, U. & Wyser, K. 2006 A 140-year simulation of European climate with the new version of the Rossby Centre regional atmospheric climate model (RCA3). *SMHI Rep. Meteorol. Climatol. 108*.

Kotlarski, S., Block, A., Böhm, U., Jacob, D., Keuler, K., Knoche, R., Rechid, D. & Walter, A. 2005 Regional climate model simulations as input for hydrological applications: evaluation of uncertainties. *Adv. Geosci.* **5**, 119–125.

Lenderink, G., Buishand, A. & van Deursen, W. 2007 Estimates of future discharges of the river Rhine using two scenario methodologies: direct versus delta approach. *Hydrol. Earth Syst. Sci.* **11**(3), 1145–1159.

Lettenmaier, D. P., Wood, A. W., Palmer, R. N., Wood, E. F. & Stakhiv, E. Z. 1999 Water resources implications of global warming: a US regional perspective. *Clim. Change* **43**, 537–579.

Lindström, G., Johansson, B., Persson, M., Gardelin, M. & Bergström, S. 1997 Development and test of the distributed HBV-96 model. *J. Hydrol.* **201**, 272–288.

Middelkoop, H., Daamen, K., Gellens, D., Grabs, W., Kwadijk, J. C. J., Lang, H., Parmet, B. W. A. H., Schädler, B., Schulla, J. & Wilke, K. 2001 Impact of climate change on hydrological regimes and water resources management in the Rhine Basin. *Clim. Change* **49**, 105–128.

Nakićenović, N., Alcamo, J., Davis, G., de Vries, B., Fenhann, J., Gaffin, S., Gregory, K., Grübler, A., Jung, T. Y., Kram, T., La Rovere, E. L., Michaelis, L., Mori, S., Morita, T., Pepper, W., Pitcher, H., Price, L., Riahi, K., Roehrl, A. & Rogner, H.-H. 2000 *IPCC Special Report on Emissions Scenarios*. Cambridge University Press, Cambridge, UK and New York, NY, USA.

Olsson, J., Berggren, K., Olofsson, M. & Viklander, M. 2009 Applying climate model precipitation scenarios for urban hydrological assessment: a case study in Kalmar City, Sweden. *Atmos. Res.* **92**, 364–375.

Roeckner, E., Brokopf, R., Esch, M., Giorgetta, M., Hagemann, S., Kornblueh, L., Manzini, E., Schlese, U. & Schulzweida, U. 2006 Sensitivity of simulated climate to horizontal and vertical resolution in the ECHAM5 atmosphere model. *J. Clim.* **19**, 3771–3791.

Trenberth, K. E. 1999 Conceptual framework for changes of extremes of the hydrological cycle with climate change. *Clim. Change* **42**, 327–339.

Vehviläinen, B. & Huttunen, M. 1997 Climate change and water resources in Finland. *Boreal Environ. Res.* **2**, 3–18.

Vrac, M., Naveau, P. & Drobinski, P. 2007 Modeling pairwise dependencies in precipitation intensities. *Nonlinear Process. Geophys.* **14**, 789–797.

Wilks, D. S. 1995 *Statistical Methods in the Atmospheric Sciences: An Introduction*. Academic Press, INC, Burlington, MA, p. 86.

Yang, W., Andréasson, J., Graham, P. L., Olsson, J., Rosberg., J. & Wetterhall, F. 2008 A scaling method for applying RCM simulations to climate change impact studies in hydrology. In: *XXV Nordic Hydrological conference Nordic Association for Hydrology Reykjavik, Iceland*, August 11–13, *Vol. 1*, pp. 256–265.

First received 22 December 2008; accepted in revised form 15 September 2009. Available online April 2010